SLAC-PROPOSAL E160
September 12, 2000

Proposal to Measure the A-Dependence of J/ψ and ψ' Photoproduction

V. Ghazikhanian, G. Igo, S. Trentalange
University of California Los Angeles, Los Angeles CA 90095

S. Bueltmann, E. Chudakov, J. Dunne
Jefferson Lab, Newport News VA 23606

R. G. Arnold, P. E. Bosted(*), R. Hicks,
G. Peterson, S. E. Rock, J. Shaw
University of Massachusetts, Amherst, Massachusetts 01003 (*) co-spokesperson (contact: Bosted@Slac.Stanford.Edu (650) 926-2319)

R. Lombard
DAPNIA-Service de Physique Nucleaire Centre d'Etudes de Saclay, F–91191 Gif/Yvette, France

G. Tamas
Institut für Kernphysik, D55099, Mainz, Germany

S. Penttila, G. Mitchell
Los Alamos National Laboratory, Los Alamos, New Mexico 87545

A. Klein, S. Kuhn, C. Hyde-Wright
Old Dominion University, Norfolk, Virginia 23529

W. Meyer, St. Goertz, G. Reicherz
Ruhr-Universität Bochum, Universitätstr. 150, Bochum, Germany

P. Decowski
Smith College, Northampton, Massachusetts 01063

P. Anthony, R. Erickson, T. Fieguth,
S. Rokni, S. St.Lorant, Z. M. Szalata, D. Walz
Stanford Linear Accelerator Center, Stanford, California 94309

D. Crabb(*), D. Day,
R. Lindgren, D. Pocanic, O. Rondon, F. Wesselmann
University of Virginia, Charlottesville, Virginia 22901 (*) co-spokesperson (contact: Dgc3q@Virginia.Edu (804) 924-6790)

T. Averett, D. Armstrong, K. Griffioen(*)
College of William and Mary, Williamsburg, Virginia 23187 (*) co-spokesperson (contact: griff@physics.wm.edu (757) 221-3537)

N. Akopov, A. Apyan, R. Avakian, A. Avetisian,
S. Darbinian, K. Ispirian, S. Taroyan
Yerevan Physics Institute, Yerevan, Armenia

Abstract

We propose to measure the A-dependence of the J/ψ and ψ' photoproduction cross sections in End Station A at SLAC using an unpolarized coherent bremsstrahlung beam (15, 25 and 35 GeV) incident on various nuclear targets. These first ever measurements of the A-dependence of ψ' photoproduction will test the claim that the ψ'-nucleon cross section is as large as 25 mb. We will improve the previous measurements of the J/ψ cross section by more than a factor of three in both statistical and systematic errors, which will allow for a significantly more reliable extraction of the J/ψ-nucleon cross section and its evolution with beam energy. This experiment is uniquely suited (1) for understanding the interplay of perturbative QCD and color transparency in the creation and interaction of J/ψ and ψ' particles in nuclei; (2) for resolving the mystery of why vector meson dominance and geometrical expectations for the J/ψ-nucleon cross section are at odds (unlike for the ρ); and (3) for constraining the possible causes of J/ψ suppression in ultra-relativistic heavy-ion collisions which produce J/ψ's with energies in the range that we will measure. SLAC is the only existing laboratory capable of making these measurements.

We request re-establishment of the coherent bremsstrahlung photon facility for End Station A, installation of the LASS dipole, and upgrades to the scintillator hodoscope arrays. We request two months of running time at 120 Hz, and two weeks of checkout time.

1 Overview

The QCD dynamics of charmonium production and the charmonium-nucleon cross sections remain poorly understood, despite three decades of experiments and corresponding theoretical work. By various accounts the J/ψ-nucleon cross section $\sigma_{\rm tot}^{\psi N}$ ranges from less than 1 mb to more than 6 mb [1, 2, 3, 4, 5, 6, 7, 8, 9], and the ψ'-nucleon cross section $\sigma_{\rm tot}^{\psi' N}$ ranges from 3 to 25 mb [7, 8, 9, 10]. The muddle is both experimental and theoretical. Because $\sigma_{\rm tot}^{\psi N}$ cannot be measured directly, one can only extract it from observables using a model. Determinations from elastic photoproduction data on the nucleon using vector meson dominance (VMD) yield $\sigma_{\rm tot}^{\psi N} \leq 1$ mb, whereas extractions from the A-dependence of J/ψ photo- and hadro-production give $\sigma_{\rm tot}^{\psi N}$ somewhere in the range 3–7 mb. In VMD a photoproduced meson of mass m must have a transverse size $\sim 1/m$ by uncertainty principle arguments. Its interaction cross section, then, should scale as $(1/m)^2$, which implies that $\sigma_{\rm tot}^{\psi' N}/\sigma_{\rm tot}^{\psi N} = (m_{J/\psi}/m_{\psi'})^2 \approx 0.7$ and $\sigma_{\rm tot}^{\psi' N}$ should be even less than 1 mb. However, by simple geometrical arguments the interaction cross section scales with transverse area, and therefore we expect $\sigma_{\rm tot}^{\psi N} = (r_{J/\psi}/r_\pi)^2 \sigma_{\rm tot}^{\pi N} = 2-5$ mb, in which $r_\pi \approx 0.65$ fm, $\sigma_{\rm tot}^{\pi N} \approx 25$ mb and $r_{J/\psi} \approx 0.2 - 0.3$ fm. Since the ψ' has roughly double the radius of the ψ, one would expect $\sigma_{\rm tot}^{\psi' N} = 8 - 20$ mb. It remains a mystery why VMD, which works well for the ρ, fails miserably for charmonium.

One plausible explanation [10] invokes color transparency: at the instant of diffractive production the J/ψ or ψ' is in a point-like configuration which has a ≈ 1 mb cross section with nucleons as VMD suggests, but this configuration rapidly evolves into a full-size J/ψ or ψ' with $\sigma_{\rm tot}^{\psi N} \approx 3 - 5$ mb and $\sigma_{\rm tot}^{\psi' N} \approx 12 - 20$ mb, respectively. At SLAC energies, one can hope to see this evolution. In this process [11, 12, 13], a photon undergoes a hard $\gamma N \to J/\psi N$ interaction with a nucleon in a nucleus. This can happen over a distance ℓ_c spanned by the lifetime of a $c\bar{c}$ fluctuation of the photon. The coherence length is estimated as $\ell_c \approx 2E_\gamma/4m_c^2 \approx 0.04 E_\gamma$ fm, with the photon energy E_γ measured in GeV. The J/ψ evolves from the point-like configuration of the hard interaction to a full on-shell physical J/ψ particle over a much longer distance ℓ_F. This formation length $\ell_F \approx 2E_{J/\psi}/2m_c(M_{\psi'} - M_{J/\psi}) \approx 0.2 E_\gamma$ fm must be small compared to the nuclear radius R_A in order for one to use standard Glauber theory to extract the physical J/ψ-nucleon cross section $\sigma_{\rm tot}^{\psi N}$ from measurements of the ratio $T(A) = \sigma_A/A\sigma_N$. The estimates of ℓ_c and ℓ_F indicate that photoproduction data in the range $8 < E_\gamma < 50$ GeV span precisely the region where the interplay between coherence and formation lengths can most dramatically influence $T(A)$.

The energies of the J/ψ's produced for $E_\gamma = 10$–50 GeV are typical of those coming from ultra-relativistic heavy-ion collisions, even though the beam energies in that case are much higher. The search at CERN and RHIC for J/ψ suppression in heavy ion collisions is generally regarded as one of the most compelling signatures for the onset of the quark-gluon plasma [14]. However, modeling this suppression requires accurate knowledge of the J/ψ-nucleon cross section, which is at present uncertain. Without a proper understanding of how ℓ_c, ℓ_F and color transparency influence $\sigma_{\rm tot}^{\psi N}$, any evidence for quark-gluon plasma formation from J/ψ suppression is weak. For example, it is quite possible that only in

collisions of large nuclei (e.g. Pb+Pb) do the J/ψ's reach their full interaction cross section, and therefore disappear at a greater rate than in smaller nuclei.

The only low-energy experiment designed to measure $T(A)$ was performed at SLAC in 1975, using an average photon energy of 17 GeV with Be and Ta targets [3]. The extracted J/ψ-nucleon cross section is $\sigma_{\rm tot}^{\psi N} = 3.8 \pm 0.8 \pm 0.5$ mb. The SLAC result at $E_\gamma = 17$ GeV, with $\ell_F \approx 3.4$ fm, provides no information on whether $\sigma_{\rm tot}^{\psi N}$ depends on ℓ_F. Moreover, experimental backgrounds were difficult to estimate accurately because only two nuclei were used, and J/ψ's were detected by the decay to only a single high p_T muon, rather than by muon pairs, which allow reconstruction of the J/ψ particles. There were no experimental signatures to separate nuclear coherent, quasi-elastic, and inelastic contributions, nor was any correction made for J/ψ's that originate from ψ' decays.

The previous SLAC experiment [3] can be improved in several ways: a) the use of four nuclei (Be, Al, Cu, Pb) rather than two to study the contributions of coherent J/ψ production and to test the assumed functional form of $T(A)$ over a wide range of A; b) measurements over a wide range of photon energies (from 15–45 GeV) which cover ℓ_c from 0.6 fm (smaller than the proton radius) to 1.8 fm (larger than the internucleon spacing in nuclei) and ℓ_F from 3.3 fm (roughly the radius of Al) to 9.9 fm (larger than the radius of Pb); c) full J/ψ reconstruction through measurement of both decay muons to minimize backgrounds and to measure the squared c.m. energy s and and the square of the four-momentum transfer t; d) higher count rates to reduce the statistical error on $\sigma_{\rm tot}^{\psi N}$ to below 0.3 mb (this requires approximately 8000 reconstructed quasi-elastic J/ψ particles per target at each kinematic point); and e) measurements of the ψ', which should have about 4 times the J/ψ-nucleon cross section, and which allows a determination of the A-dependence of the J/ψ's coming from ψ' decays (the branching ratio of $\psi' \to J/\psi$ is 54%).

Existing photoproduction experiments have collected samples on the order of a thousand events or less. This proposal would increase the total number of photoproduced J/ψ's by almost an order of magnitude. By contrast, the hadroproduction experiments typically have much larger sample sizes (from 50,000 to 100 million), but reaction mechanisms are harder to disentangle.

The high statistics of this proposal will permit a detailed study of the $s-$ and $t-$ dependence of coherent, quasi-elastic and inelastic J/ψ and ψ' photoproduction from a nucleon. It will also make possible a detailed study of the A-dependence of inelastic production over a range of coherence lengths ℓ_c both smaller and larger than the size of a nucleon. This can shed light on the question of whether nuclei have enhanced gluon distributions or whether J/ψ production can occur in nuclei by gluon exchanges from multiple nucleons [15].

SLAC is uniquely capable of making this measurement on a time scale to be of use in interpreting the relativistic heavy-ion experiments currently underway at RHIC and CERN. This proposal is complementary to one at Jefferson Lab designed to measure J/ψ photoproduction from below threshold to 11 GeV [16].

2 Motivation

The motivations for this proposal are:
1) to study the interplay of perturbative QCD and color transparency in the creation and interaction of J/ψ and ψ' particles in nuclei;
2) to understand the mismatch between the vector meson dominance (VMD) and geometrical expectations for the J/ψ-nucleon cross section $\sigma_{\rm tot}^{\psi N}$;
3) and to constrain the possible causes of J/ψ suppression in relativistic heavy-ion collisions.

These three topics are naturally related to each other. Although coherence and formation lengths are general properties of the photoproduction of vector mesons, there are at present no data that meaningfully constrain the models for these quantities. What is the size of the meson at the point of momentum transfer with the nucleon? How quickly does it expand to become a normal hadron? Does this reduced size imply a reduced cross section with nuclear matter (color transparency)? What is the source of the discrepancy between the VMD determinations of $\sigma_{\rm tot}^{\psi N}$ and the simple geometrical arguments that cross sections should scale as the square of the particle radius? This proposal addresses these questions.

We will determine:
1) t-distribution parameters for coherent, quasi-elastic, and inelastic photoproduction of ψ and ψ' for $E_\gamma = 15$, 25 and 35 GeV. Any change in these values as a function of beam energy or nuclear size would indicate a change in reaction mechanism, say from 2 gluon exchange to more exotic manifestations of the QCD gluon van der Waals potential [17]. At present, elastic data for beam energies below about 100 GeV give quite different exponential slopes than the higher-precision high-energy HERA experiments.
2) total photoproduction cross sections for coherent, quasi-elastic, and inelastic photoproduction of J/ψ and ψ'. These data will allow the determination of $\sigma_{\rm tot}^{\psi N}$ and $\sigma_{\rm tot}^{\psi' N}$ as well as the initial premeson sizes at the point of momentum transfer with the nucleon, and test claims that $\sigma_{\rm tot}^{\psi' N}$ could be as large as 25 mb.
3) A-dependence exponents α for coherent, quasi-elastic, and inelastic photoproduction by fitting the cross sections to $\sigma_A = \sigma_0 A^\alpha$. At the very least (especially for the ψ') α should depend strongly on energy if the above picture is correct. More likely, the data will not scale as a power law in A because of the interplay of ℓ_c, ℓ_F and color transparency.

3 Cross Sections for J/ψ and ψ'

Following the discovery of the J/ψ, a number of photoproduction measurements were made in the 1970's. These were extended to higher beam energies in the 1980's, and have culminated in recent high-energy data from the HERA *ep* collider experiments. Table 1 summarizes the existing measurements of J/ψ photoproduction on nucleon targets.

During the 1980's and 1990's a number of high-energy hadron production measurements were made using a variety of probes and nuclear targets in an effort to understand production of J/ψ's in heavy-ion reactions. Table 2 lists the various experiments which have measured the A-dependence of J/ψ production, including two real-photon experiments.

Table 1: Various experimental determinations of J/ψ photoproduction on the nucleon.

date	reference	experiment	beam	energy	target	state
1975	Martin[18]	SLAC	γ	18.2 GeV	p, d	J/ψ
1975	Knapp[2]	FNAL	γ	50–200 GeV	Be	J/ψ
1975	Gittelman[19]	Cornell	γ	11 GeV	Be	J/ψ
1975	Camerini[1]	SLAC	γ	13–21 GeV	p, d	$J/\psi, \psi'$
1976	Nash[20]	FNAL	γ	31–80 GeV	d	J/ψ
1977	Anderson[3]	SLAC	γ	17 GeV	Be, Ta	J/ψ
1982	Binkley[21]	FNAL	γ	60–300 GeV	p, d	J/ψ
1984	Denby[22]	FNAL	γ	105 GeV	p	J/ψ
1986	Sokoloff[4]	FNAL E691	γ	120 GeV	p, Be, Fe, Pb	J/ψ
1987	Barate[23]	CERN NA14	γ	90 GeV	^{6}Li	$J/\psi, \psi'$
1993	Frabetti[24]	FNAL E687	γ	100–375 GeV	Be	J/ψ
1997	Breitweg[25]	HERA ZEUS	e	850–32400 GeV	p	J/ψ
2000	Aldoff[26]	HERA H1	e	360–43300 GeV	p	$J/\psi, \psi'$

Table 2: Various experimental determinations of the A-dependence of J/ψ production.

date	reference	experiment	beam	energy	target	state
1977	Anderson[3]	SLAC	γ	17 GeV	Be, Ta	J/ψ
1983	Badier[27]	CERN NA3	$\pi^\pm, K^\pm, p^\pm$	150–280 GeV	H, Pt	J/ψ
1986	Sokoloff[4]	FNAL E691	γ	120 GeV	H, Be, Fe, Pb	J/ψ
1988	Katsanevas[28]	FNAL E537	$\bar{p}, \pi^-$	125 GeV	Be, Cu, W	J/ψ
1990	Kartik[29]	FNAL E672	π^-	530 GeV	C, Al, Cu, Pb	J/ψ
1991	Alde[30]	FNAL E772	p	800 GeV	D, C, Ca, Fe, W	$J/\psi, \psi'$
1999	Alexandrov[31]	CERN WA92	π^-	350 GeV	Si, Cu, W	$J/\psi, \psi'$
1999	Abreu[7]	CERN NA38	p, O, S	200,450 GeV	p, d, C	$J/\psi, \psi'$
		NA51			Al, Cu, W, U	
2000	Tribble[32]	FNAL E866	p	800 GeV	Be, Fe, W	$J/\psi, \psi'$

3.1 Determining $\sigma_{\rm tot}^{\psi N}$ using A-dependence

The first extraction of the J/ψ-nucleon cross section was done at SLAC in the 1970's [3] using beryllium and tantalum targets and a bremsstrahlung beam of 20 GeV. The yield of single muons was detected at a transverse momentum of 1.65 GeV where the backgrounds from Bethe-Heitler pairs and muons from the decay of hadrons were small. The data were corrected for coherent production which depends on the nuclear form factor, and the effects of nucleon motion and the Pauli exclusion principle, calculated in a Fermi gas model. The quantity $\sigma_{\rm tot}^{\psi N} = 3.5 \pm 0.8$ mb was calculated using a simple nuclear-optics model.

Gerschel and Hüfner [5] have tried to extract the J/ψ-nucleon cross section from the A-dependence of J/ψ production for a number of experiments using hadron and photon beams. The cross section ratio was expressed as $\sigma^{pA\to\psi}/A\sigma^{pN\to\psi} = \exp(-L\rho_0\sigma_{\rm tot}^{\psi N})$, in which L is the length of the absorption trajectory through the nucleus, and ρ_0 is the nuclear density. They find consistent results with $\sigma_{\rm tot}^{\psi N} = 6.2 \pm 0.3$ mb. This analysis assumes an instantaneous creation of the J/ψ, and is much larger than the SLAC result. Abreu, *et al.* [7] analyzed the data of NA51 and NA38 using the same technique and have obtained $\sigma_{\rm tot}^{\psi N} = 5.9 \pm 0.6$ mb and $\sigma_{\rm tot}^{\psi' N} = 24 \pm 5$ mb.

Recent data from Fermilab E866 on the nuclear dependence of J/ψ and ψ' production have been analyzed by He, Hüfner and Kopeliovich [9] in a model in which a premeson is created instantaneously and then is absorbed according to a time and energy-dependent effective cross section

$$\sigma_{\rm abs}^{\psi N}(\tau, \sqrt{s_{\psi N}}) = \{\sigma_\infty + (\sigma_0 - \sigma_\infty)\cos(\Delta M \tau)\} \left(\frac{\sqrt{s_{\psi N}}}{10\text{GeV}}\right)^\lambda \tag{1}$$

in which σ_∞ and σ_0 are parameters to be determined from the data, ΔM is the mass difference between the J/ψ and ψ', τ is the elapsed time, and $s_{\psi N}$ is the squared center-of-momentum energy of the reaction. The energy dependence ($\lambda = 0.4$) was determined from photoproduction experiments. With appropriate corrections for ψ' decays into J/ψ, the cross sections for fully-developed charmonium states are $\sigma_{\rm tot}^{\psi N} = 2.8 \pm 0.3$ mb and $\sigma_{\rm tot}^{\psi' N} = 10.5 \pm 3.6$ mb for a charmonium-nucleon c.m. energy of 10 GeV. These numbers scale roughly geometrically as the square of the rms radii $\sqrt{\langle r^2_{J/\psi}\rangle} = 0.42$ fm and $\sqrt{\langle r^2_{\psi'}\rangle} = 0.85$ fm. The extracted premeson cross sections σ_0 are in the range of 3-4 mb, indicating that at least for the ψ' there is a significant expansion of the initial $c\bar{c}$ state as it propagates through the nucleus. The premeson cross section for the J/ψ cannot be disentangled from χ_c decays into J/ψ, and so the number remains only suggestive. With a real photon beam, however, χ_c production should be suppressed because, unlike the J/ψ and ψ', its quantum numbers are different from the photon.

A recent calculation [8] using the light-cone dipole formalism predicts similar but slightly larger values at $\sqrt{s} = 10$ GeV:

$$\sigma_{\rm tot}^{\psi N} = 3.56 \pm 0.08 \text{ mb} \qquad \text{and} \qquad \sigma_{\rm tot}^{\psi' N} = 12.19 \pm 0.61 \text{ mb} \tag{2}$$

3.2 Determining $\sigma_{\rm tot}^{\psi N}$ using Vector Meson Dominance

As early as 1975, Camerini, *et al.* [1] determined the J/ψ-nucleon cross section using photoproduction data from hydrogen and deuterium targets using a simple vector meson dominance (VMD) model. They found that $\sigma_{\rm tot}^{\psi N} \leq 0.8$ mb, which is surprisingly small.

Hüfner and Kopeliovich [6] have extended the usual VMD analysis of $\gamma N \to \psi N$ data to include a superposition of charmonium states. The multi-channel case is related to the VMD amplitude for elastic production by $f(\gamma N \to \psi N) = N_\psi(Q^2) f_{\rm VMD}(\gamma N \to \psi N)$ in which they estimate $N_\psi(0) = 0.30$ and 0.064 for the J/ψ and ψ', respectively. This brings the ratio $\sigma_{\rm tot}^{\psi' N}/\sigma_{\rm tot}^{\psi N}$ to 3.75 which is more in line with QCD expectations, and 2.8 ± 0.1 mb $< \sigma_{\rm tot}^{\psi N}(\sqrt{s} = 10$ GeV $) < 4.1 \pm 0.2$ mb, which is about a factor of three larger than previous VMD predictions. The errors on the values come from the experimental input, and the range of values comes from the theoretical uncertainties.

Given the large uncertainties in the VMD extractions, it is clearly important to supplement the photoproduction data on the nucleon with high-quality data on a variety of nuclear targets.

3.3 A Simple Model Inspired by Existing Data

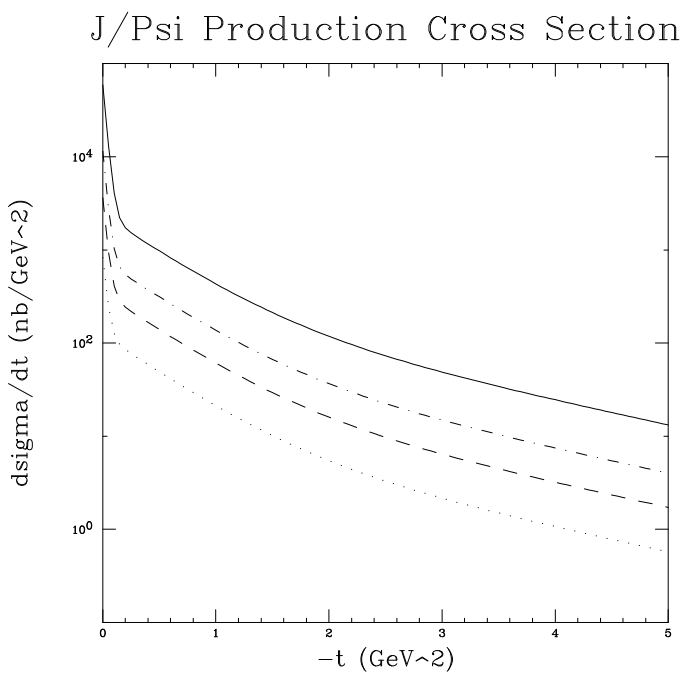

Figure 1: Estimates of $d\sigma/dt$ (nb/GeV^2) for Be (dotted), Al (dashed), Cu (dot-dashed), and Pb (solid) at a photon energy of 20 GeV using the simple model described in the text. Three exponential slopes corresponding to coherent, quasi-elastic and inelastic scattering can be seen from the plot.

The nature of the A-dependence of incoherent production is still quite poorly understood. We can use existing experimental data as shown in Table 3 to make a simple model for counting-rate estimates. The incoherent cross section has been parameterized as

$$\sigma_{\rm incoh} = \sigma^0_{\rm incoh} A^{\alpha_{\rm incoh}} \tag{3}$$

with $\alpha_{\rm incoh}$ fit to the data of various experiments. The SLAC experiment by Anderson, *et al.*, [3] looked at only two nuclei, Be and Ta. From their cross section ratios one obtains $\alpha_{\rm SLAC} = 0.94 \pm 0.03$. This agrees with a value of $\alpha_{\rm FNAL} = 0.94 \pm 0.02 \pm 0.03$ measured at Fermilab using 120 GeV photons and four targets, H, Be, Fe and Pb. By contrast, the cross section ratios for Fe versus H and D, measured with 250-280 GeV μ^+ beams by the European Muon Collaboration [33] (EMC) yields $\alpha_{\rm EMC} = 1.10 \pm 0.03 \pm 0.04$. The errors quoted are statistical followed by systematic. The SLAC and FNAL measurements are primarily quasi-elastic, but corrections for inelastic scattering in the data are schematic at best. Moreover, $\alpha_{\rm FNAL}$ varies by 10% for p_T^2 less than and greater than 1 GeV^2. The EMC data are primarily inelastic and have been used as evidence for an enhanced gluon distribution in nuclei. Clearly, a significant improvement in the precision of these extractions is warranted.

Using the available data as a guide, a simplified model of J/ψ photoproduction can be constructed for rate estimates.

$$\frac{d\sigma}{dt} = \sigma(A^{\alpha_{\rm coh}} r_{\rm coh} a e^{at} + A^{\alpha_{\rm elas}} b e^{bt} + A^{\alpha_{\rm inel}} r_{\rm inel} c e^{ct}) \tag{4}$$

in which the three terms correspond to coherent, quasi-elastic, and inelastic production. The coefficients are determined as follows:

- $\alpha_{\rm coh} = 1.4$ — From Sokoloff, *et al.* [4].
- $\alpha_{\rm elas} = 0.94$ — This ignores the results of Ref. [33] in favor of Refs. [3, 4] which agree with each other.
- $\alpha_{\rm inel} = 1$ — This is suggested by $\alpha_{\rm elas}$ approaching unity for large p_T^2 in Ref. [4], but it could be greater than unity as observed by Ref. [33].
- $r_{\rm coh} = 0.14$ — The ratio of coherent to incoherent scattering is given in Ref. [4] for 120 GeV photons.
- $r_{\rm inel} = 0.30$ — Although this ratio should decrease at lower beam energies according to the calculations of Berger and Jones [34], we take the averages quoted in Refs. [21, 22] for beam energies in the range 60-300 GeV as a conservative upper bound.
- $a = 33$ GeV^{-2} — Although this coefficient most likely has some A-dependence, we simply take the average of $a_{\rm Be} = 40$ from Ref. [2], $a_{^6{\rm Li}} = 25.0 \pm 2.3$ from Ref. [22], and $a_{\rm Fe,Pb} = 33$ from Ref. [4].

- $b = 2.0$ GeV^{-2} — This is the average of four measurements below about 100 GeV: 1.25 ± 0.20 from Ref. [19], 2.9 ± 0.3 from Ref. [1], 1.8 ± 0.4 from Ref. [20], and 2.5 ± 0.2 from Ref. [23], which yields 2.04 ± 0.24.

- $c = 0.6$ GeV^{-2} — Taken from Barate, *et al.*[23].

The cross section σ has been parameterized by Hüfner and Kopeliovich [6] as

$$\sigma(\gamma N \to J/\psi N) = (10.3 \pm 0.7 \text{ nb}) \left[\frac{\sqrt{s}}{10 \text{ GeV}} \right]^{0.80 \pm 0.04} \tag{5}$$

We fully expect that the actual data will show a dependence of α on beam energy for the three processes as color transparency plays a larger role in the propagation of J/ψ's through nuclear matter. Fig. 1 shows the estimated J/ψ photoproduction cross sections for Be, Al, Cu, and Pb using this model. Coherent production is confined to a region $-t < 0.2$ GeV^2; quasi-elastic production dominates up to about $-t = 2$ GeV^2; and inelastic production prevails above $-t = 2$ GeV^2.

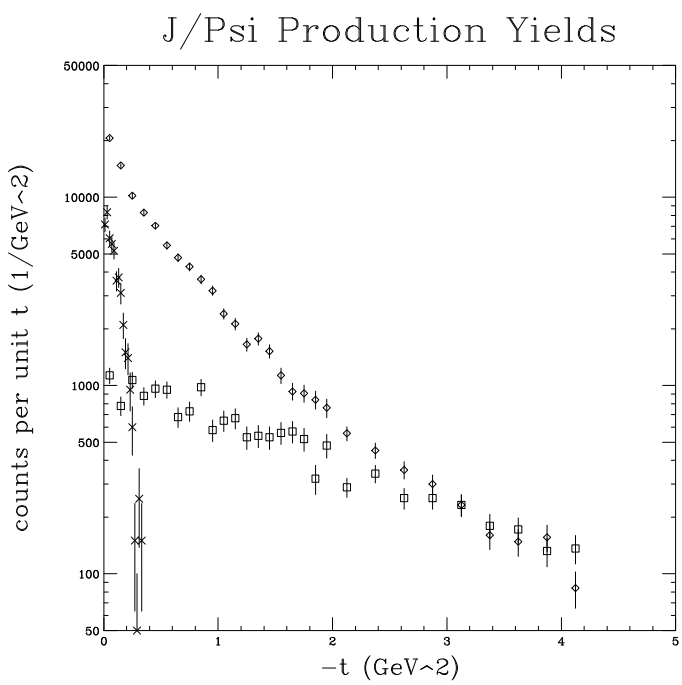

Figure 2: Simulated counts per GeV^2 as a function of $-t$ assuming an experimental t-resolution of 0.1 and 8000 recorded quasi-elastic events, 1000 coherent events, and 2000 inelastic events. This is in the rough proportion expected for the targets and energies of this experiment. The diamonds are the full simulated data; the coherent component (x's) drops off rapidly by about $-t = 0.3$ GeV^2; the inelastic component is small, but underlies the others (squares).

Fig. 2 shows a Monte Carlo simulation of the expected t-distributions for 8000 quasi-elastically produced J/ψ's. Clearly, the region $0.3 < -t < 2$ GeV^2 is dominated by the

quasi-elastic production, and contains about 55% of the quasi-elastic events. About 43% of the quasi-elastic events lie below $-t = 0.3$ GeV^2 and 2% lie above $-t = 2$ GeV^2. The detector resolution flattens the observed exponential slope for quasi-elastic events from 2.0 down to about 1.7; therefore, the data will be first corrected for resolution before extracting individual cross sections. With roughly 4000 events with $0.3 < -t < 2$ GeV^2, we expect a statistical error of 1.6% for this region. A simple integration of the fitted exponential yields a 3% error for the integrated cross section. This is comparable to the systematic errors in measuring integrated beam current, target thickness, detector acceptances, etc.

Table 3: Observations from J/ψ photoproduction experiments.

k (GeV)	ref.	sample	$\sigma_{\rm tot}^{\psi N}$	a GeV^{-2}	b GeV^{-2}	c GeV^{-2}
11	Gittelman	540			1.25 ± 0.20	
13–21	Camerini	1200	< 0.8 mb		2.9 ± 0.3	
20	Anderson	Be: 2700	3.5 ± 0.8 mb			
		Ta: 800				
55	Nash	24			1.8 ± 0.4	
50–200	Knapp	60	≈ 1 mb	Be: 40		
60–300	Binkley	d: 1650				
		p: 175				
90	Barate	J/ψ: 1272		^{6}Li: 25.0 ± 2.3	2.5 ± 0.2	0.62 ± 0.20
		ψ': 23				
105	Denby	430				
120	Sokoloff	p: 310	1–2 mb	Fe,Pb: 33		
		Be: 510				
		Fe: 240				
		Pb: 94				
100–375	Frabatti	290				
200, 450	Abreu		J/ψ: 6.4 ± 0.8 mb			
			ψ': 24 ± 5 mb			
360–	H1 (96)	400			$4.0 \pm 0.2 \pm 0.2$	$1.6 \pm 0.3 \pm 0.1^\dagger$
43,300						$0.39 \pm 0.06 \pm 0.03$
	H1 (98)	ψ': 80				
	H1 (00)	el: 1000			4.73 ± 0.25	
850–	ZEUS (97)	el: 621			4.6 ± 0.4	$\approx 1^\dagger$
32,400		inel: 364				$0.32 \pm 0.03 \pm 0.01$

†Dissociative production

We have used this simple model for rate estimates, in which we assume an average nuclear target for which coherent scattering is 10% and inelastic scattering is 20% of the total J/ψ yield. Table 4 lists the expected statistical accuracy for the case of 8000 quasi-elastic J/ψ's in the sample. For the 15 GeV beam energy (2000 quasi-elastic J/ψ events) these errors will be roughly twice as large. Errors were estimated as follows: A Monte Carlo sample as shown in Fig. 2 was generated and fit to the sum of three exponentials. The associated errors on the exponential slopes are given as a, b, and c. The total quasi-elastic cross section can be obtained by measuring the data in the range $0.3 < -t < 2$ GeV^2

and scaling by the calculated fraction (55%) of quasi-elastic events within this t interval using b. The total inelastic cross section is determined in the same way with the fraction in the interval $2 < -t < 4$ GeV^2 of 30%. Since the coherent events ride on a large quasi-elastic background, a subtraction is required of 4000 ± 80 events (determined from the quasi-elastic analysis) from the total of 5000 ± 71 events. The A-dependence, however, can be determined more accurately than the absolute cross sections because the whole t range need not be covered. Errors are large for the coherent process because there is no region of t in which the coherent scattering is the only contribution. However, events are almost exclusively quasi-elastic and inelastic in the regions $0.3 < -t < 2$ and $2 < -t < 4$ GeV^2, respectively. The errors on α were determined from the error in the fit of four nuclei to the form σA^{α}. The ψ' sample of 200 quasi-elastic events is somewhat smaller, and the errors on $\alpha_{\psi'}$ are correspondingly larger. However, this accuracy is sufficient to see the marked change in $\alpha_{\psi'}$ expected [13] for the photon beam energy range from threshold to 50 GeV. Errors on $\sigma_{\rm tot}^{\psi N}$ and $\sigma_{\rm tot}^{\psi' N}$ were calculated assuming the simple form $\sigma_{\gamma A}/A\sigma_{\gamma N} = \exp(-L\rho_0\sigma_{\rm tot}^{\psi N})$. Then $(\sigma_{\gamma Pb}/207)/(\sigma_{\gamma Be}/9) = \exp(-(L_{Pb} - L_{Be})\rho_0\sigma_{\rm tot}^{\psi N})$ in which $\sigma_{\gamma Pb,Be}$ are measured in the range $0.3 < -t < 2$ GeV^2.

Fig. 3 shows the striking energy-evolution of $T(A)$ for J/ψ and ψ' as predicted in [13]. The simulated data show the statistical precision possible for this measurement.

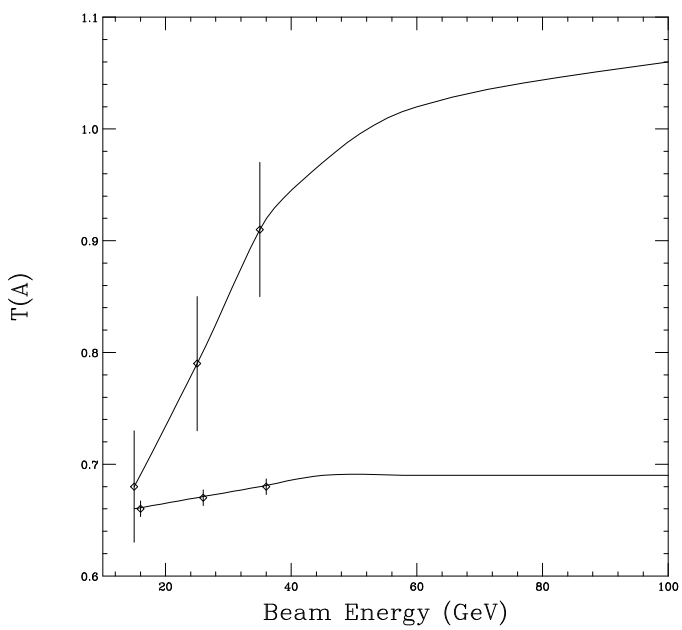

Figure 3: Predictions[13] for T(A) using a Pb target together with simulated data showing the statistical precision expected. The upper curve is for ψ' and the lower curve is for J/ψ.

Table 4: Expected statistical accuracy of various measured parameters assuming the simple 3-component model and 10,000 J/ψ events.

quantity	variable	statistical error
slope of coherent t-distribution	a	± 1 GeV^{-2}
slope of quasi-elastic t-distribution	b	± 0.04 GeV^{-2}
slope of inelastic t-distribution	c	± 0.2 GeV^{-2}
total coherent production cross section	$\sigma^{\rm tot}_{\rm coh}$	11%
total quasi-elastic J/ψ production cross section	$\sigma^{\rm tot}_{\rm elas}$	3%
total inelastic J/ψ production cross section	$\sigma^{\rm tot}_{\rm inel}$	12%
coherent A-dependence	$\alpha_{\rm coh}$	± 0.044
quasi-elastic A-dependence	$\alpha_{\rm elas}$	± 0.004
inelastic A-dependence	$\alpha_{\rm inel}$	± 0.017
ψ' A-dependence	$\alpha_{\psi'}$	± 0.044
J/ψ-nucleon cross section	$\sigma^{\psi N}_{\rm tot}$	± 0.3 mb
ψ'-nucleon cross section	$\sigma^{\psi' N}_{\rm tot}$	± 3 mb

4 Experimental Overview

Photon beams will be created using bremsstrahlung from diamond radiators. With suitable orientation, coherent peaks from the diamond are superimposed on the normal $\Phi = dk/k$ bremsstrahlung spectrum. J/ψ and ψ' particles will be identified through their decay into two muons. Just beyond the nuclear targets, the muons pass through a thick absorber that stops most pions and kaons before they can decay to muons. The muons are then tracked through a large aperture dipole. Quasi-elastic photoproduction is separated from inelastic production using the total energy of the muon pair. Those with energy near the endpoint of the bremsstrahlung spectrum are mainly quasi-elastic, as are those in the coherent bremsstrahlung peaks. The spectrometer resolution is sufficient to separate J/ψ and ψ' particles. The acceptance for J/ψ decreases from over 60% at 35 GeV to about 10% at 14 GeV.

The maximum luminosity is limited to about 5×10^{10} photons/sec on a 1 b^{-1} target by the maximum detector rates that are tolerable with the 10^{-4} duty factor of SLAC. The plan is to make measurements at photon energies 15, 25, and 35 GeV. At 25 and 35 GeV, we will reconstruct about 8000 J/ψ clean quasi-elastic events and 200 ψ' events on each of four targets. At 15 GeV, we will collect about 2000 J/ψ events on two nuclear targets. The t-dependence of the cross sections will be fit to separate the coherent and incoherent contributions, and the A-dependence of each will be determined with very good accuracy for the J/ψ events, allowing the J/ψ quasi-elastic photoproduction cross section to be determined with statistical and systematic errors of 3% and 4%. The statistical error on the ψ' photoproduction cross section will be much larger (about 10%), but small enough to distinguish models that predict a large cross section (of order 20 mb) from predictions in the few mb range.

5 Photon Beam

5.1 Introduction

We propose to use coherent bremsstrahlung to generate the photon beam. Coherent bremsstrahlung is strongly favored in comparison with incoherent bremsstrahlung because it provides a better signal to noise ratio when considering the total rate of muons impinging on our detectors. The total muon rate per beam spill is the limiting factor on beam luminosity, rather than the current from the accelerator, so the choice of coherent bremsstrahlung offers a significant advantage.

We have rejected the Compton laser backscattering and tagged photon alternatives because they cannot provide nearly enough intensity given the SLAC beam emittance and duty cycle.

5.2 Electron and Photon Beams in the A-line

The use of coherent bremsstrahlung at SLAC was successfully demonstrated in experiment E78 [35], and we plan to use a very similar setup. A schematic layout of the photon beam line is shown in Fig. 4, and a summary of the properties of the electron and photon beams is given in Table 5. We will use the SLAC electron beam at energies of about 26, 43, and 48 GeV at currents of 1×10^{10} to 2×10^{10} electrons per 500 ns long beam pulse. We assume the accelerator will be operating in the SLED mode, at a nominal repetition rate of 120 Hz. It is not necessary to use the polarized source for this experiment.

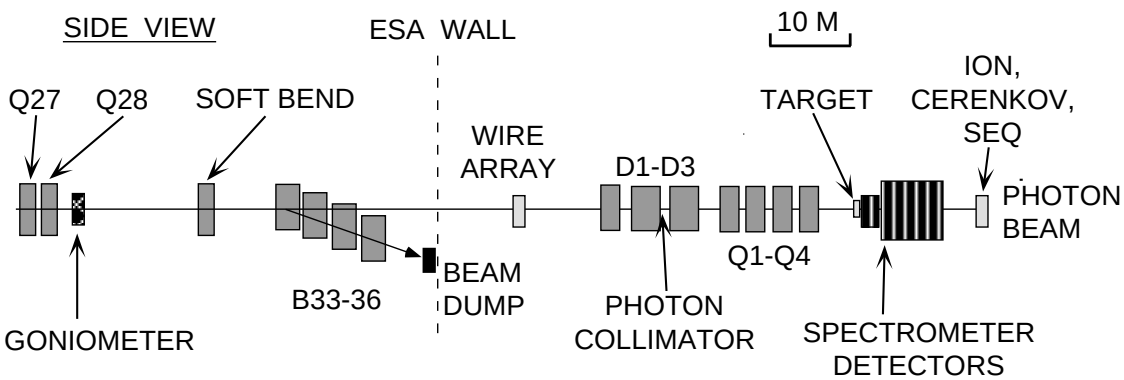

Figure 4: Overall view of the main components of the photon beam (horizontal scale is approximate, vertical scale is exaggerated). The Wire Array, D1-D3 dipole magnets, and Q1-Q4 quadrupoles are part of the current E158 setup.

For most of the running, the electrons will be incident on an existing 0.0007 radiation length (r.l.) thick oriented diamond crystal with a tilt angle θ_0 of a few milliradians. The diamond will be positioned using the SLAC goniometer [36], which can hold two radiators, and position either of them at well-defined angles with respect to the beam axis, in steps

of 25 μrad. The goniometer will be located just downstream of the Q27/Q28 quad pair at the end of the A-line, as in SLAC E78 [35].

We plan to reduce the thickness of the two existing thicker diamond crystals to 0.0007 r.l., to be used as spares. This thickness gives the best tradeoff between photon flux and coherent peak width. The current and integrated luminosity are well below those used in E78 [35], so that it is unlikely that both diamonds in the goniometer will fail due to radiation damage or shock stresses.

The A-line quadrupoles will be adjusted to give a beam spot size of at least 10 mm^2 at the diamond to avoid overheating. The quadrupoles will also be adjusted to give a small waist at the position of the collimator. For energies below 35 GeV, it is possible to obtain spot sizes smaller than 0.7 mm by 0.7 mm. At 48 GeV, the beam will be wider in the horizontal direction (about 1.5 mm) due to the increased energy spread from synchrotron radiation in the A-line, which grows at the fifth power of beam energy. We have verified that the desired optics can be obtained without quadrupoles Q30 and Q38, which will be positioned after the goniometer and not used in this experiment.

Tuning of the electron beam spot size will be done by sending the beam at low repetition rate (10 Hz or less) and low current into End Station A and using the beam position monitors, screens, and the wire array built for E158.

To obtain photon beams, the electrons will be bent into a dump using the existing B33-36 dipole magnets, which will need to be refurbished for this experiment. Just upstream of B33, we plan to place a weak magnet with a total field strength of 0.1 kG-m. This bends 48.5 GeV electrons by 0.2 mr. The purpose of the initial soft bend is to minimize the number of energetic synchrotron radiation photons impinging upon the target 110 m downstream. The B33-B36 dipoles are not strong enough to bend electrons with $E > 25$ GeV into the existing high power dump. Therefore we will move the magnets to accommodate a smaller bend angle, and use a smaller 20 kW dump for the electrons, positioned downstream of and below the Q38 quadrupole. This will require modifying the vacuum chambers of the magnets.

5.3 Photon Beam in End Station A

After entering the End Station, the beam passes through a 3 mm diameter, 70 r.l. tungsten collimator to limit the transverse position and angle of the photons. About 30% to 90% of the photons will hit the collimator (depending on energy), corresponding to a maximum power into the collimator of 20 W for the 0.0007 r.l. diamond radiator. A four-quadrant, tungsten pin-cushion shower-emission detector as used in E78 [37] will be placed just in front of the collimator, and the beam will be centered by matching the signals in the left/right and up/down pairs.

Assuming that the existing E158 setup is in place, we plan to place the collimator between the D2 and D3 magnets. The E158 D3 dipole magnet will be powered to provide a sweeping field of 36 kG-m. This magnet will sweep charged particles produced in the collimator by an angle of at least 30 mr. A thick lead wall just in front of the target, with a 1 cm hole for the photon beam, will be used to absorb charged and neutral particles not

already absorbed by quadrupoles Q1-Q4.

Electron Energy (GeV)	26.7	43.3	48.3
Electron Current (10^{10}/spill)	2.0	1.2	1.0
Peak Photon Energy (GeV)	15.0	25.0	35.0
Linear Polarization	0.69	0.69	0.48
J/ψ per day total	1494.	9755.	10025.
J/ψ per day in Peak	423.	2988.	3713.
J/ψ goal per target	2000.	8000.	8000.
days (at 100% efficiency)	9.5	10.7	8.6

Table 5: Summary of the beam parameters, J/ψ rates, and running time needed for each of the three beam energies, assuming a 0.0007 r.l. diamond, 3 mm diameter collimator, average 1 b^{-1} target thickness, and the spectrometer described below. The linear polarization value is at the main coherent peak.

The photon beam, after passing through the target and muon spectrometers, will be finally stopped in a secondary emission quantameter (SEQ), used to measure the total photon beam intensity (intensity is energy-weighted flux). Just upstream of the SEQ we will use two auxiliary detectors to monitor the beam flux: an ionization chamber and an atmospheric gas Čerenkov detector. All of these standard devices will be similar to those used in E78.

As in E78, the goniometer angles will be calibrated by mapping out the ratio of flux (number of photons) compared to intensity (energy-weighted flux) as a function of horizontal and vertical angles. Maxima in the ion chamber to SEQ ratios occur at well-defined settings, and can be used to determine the correct orientation of the crystal for the desired experimental settings [35, 38].

5.4 Calculations of Photon Beam Flux and Polarization

We have calculated the photon beam flux and intensity profile using the formulas given in Eq. 35 of Ref. [39], as implemented in a Monte Carlo simulation following the very clear introduction to the practicalities of coherent bremsstrahlung given in [40]. We use the same crystal orientation as in [35] for the present calculations. For each electron beam energy, we adjust the angle θ_0 such that the discontinuity (spike) of the lowest energy coherent peak is at a value of k_0/E between 0.6 and 0.75. With no collimation, there is a long tail extending to lower energies. This tail is reduced by the collimator, as originally proposed in Ref. [41]. The incoherent tail is also reduced by collimation, but in this case the reduction is independent of photon energy. A Monte Carlo program was used to fold in the effects of multiple scattering in the radiator, beam emittance, crystal mosaic spread, and beam spot size as a function of energy. The code was checked against spectra measured in [35], and gives very good agreement with these data. The calculated intensity spectra for the three electron beam energies are shown in Fig. 5. The incoherent contribution is shown as

the dashed line. In addition to the main spike, smaller spikes at higher energies are always present in a well-defined intensity ratio.

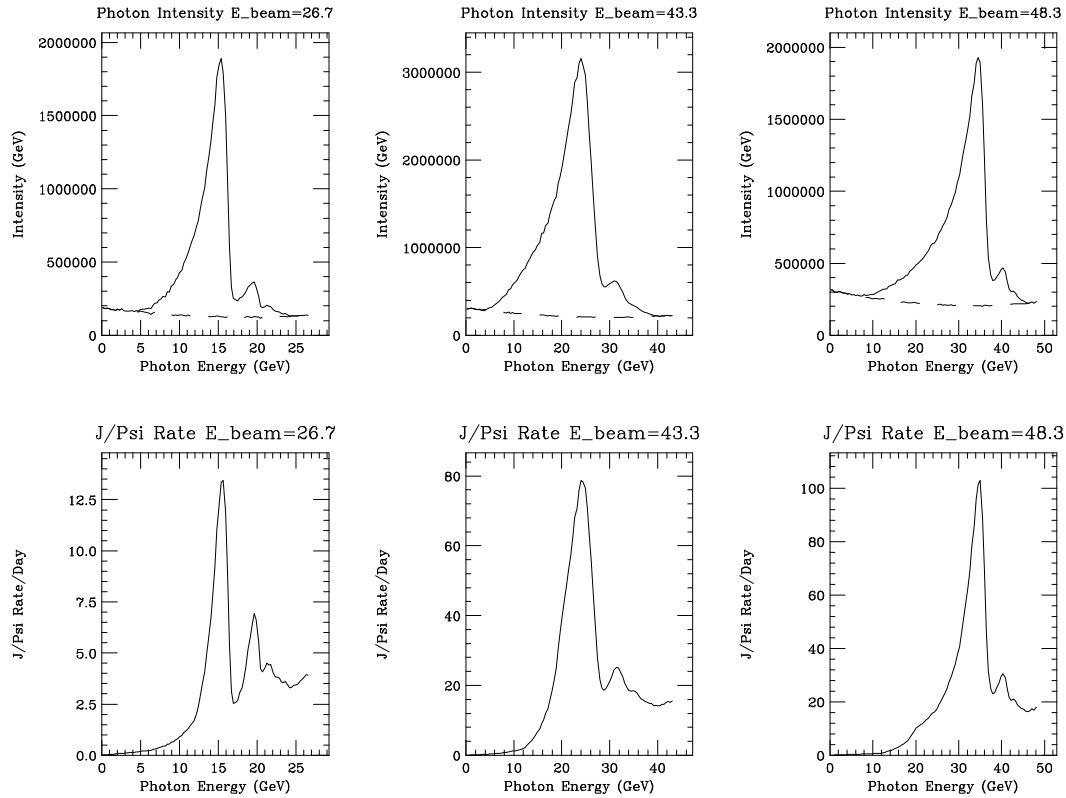

Figure 5: Upper plots are the calculated intensity (flux times energy) for collimated coherent bremsstrahlung at the three settings detailed in Table I. The dashed lines are incoherent radiation only, while the solid lines include coherent contributions. The lower plots show the corresponding rate of quasi-elastic J/ψ events as a function of photon energy.

Although it is not specifically needed for this experiment, there is a bonus with coherent bremsstrahlung that the coherent peak has a high degree of linear polarization. The axis of the polarization can be rotated by 90 degrees depending on the crystal orientation. As listed in Table 5, the degree of polarization is relatively large.

5.5 Measurements of Photon Beam Flux

We will measure the photon flux as a function of energy using pairs of Bethe-Heitler muons produced in the target and measured in our detectors. Using the formulas of [42], we find that the rate is completely dominated by elastic and quasi-elastic production, for which the sum of the muon energies is equal to the photon energy. We will detect between 10^7 and 10^8 muon pairs per day, so that the statistical error will be very small. Indeed, the high rate of Bethe-Heitler muon pairs is the limiting factor in the luminosity that can be used for the high Z targets.

Table 6: Properties of the four solid targets.

element	Z	A	ρ (g/cm^3)	g/cm^2	cm	rad. lengths	int. lengths	b^{-1}
Be	4	9.012	1.848	3.26	1.764	0.050	0.043	1.96
Al	13	26.980	2.700	3.36	1.245	0.140	0.032	2.02
Cu	29	63.546	8.960	2.57	0.287	0.200	0.019	1.55
Pb	82	207.200	11.350	1.27	0.112	0.200	0.007	0.77

6 Target

Four solid targets of roughly 1 b^{-1} thickness will be used to span the range A = 9–207. These will be mounted on a movable target ladder. Table 6 lists the properties of each target. Thicknesses were chosen to obtain up to 2 b^{-1} without exceeding 0.2 radiation lengths.

7 Spectrometer, Detector and Electronics

7.1 Introduction

The challenge in identifying J/ψ and ψ' mesons at low photon energies is the small ratio of J/ψ to total hadronic cross section (only 1 in 100,000 at 15 GeV). The SLAC duty factor of $< 10^{-4}$ makes it impossible to meet our goal of detecting hundreds of ψ mesons per day unless detectors can be made insensitive to the vast majority of particles from typical hadronic interactions. This was done in the previous SLAC experiments using small solid angle magnetic spectrometers. However, a better approach is to filter out all particles that are not muons, and reconstruct J/ψ (ψ') mesons through the 6% (1%) branching ratio to muon pairs. Using a spectrometer based on the large LASS dipole, this approach gives more than a factor of ten higher rates, and is especially useful for photon energies above 30 GeV, where almost half of all the muon pairs are detected. Another advantage of having a hadronic filter close to the target is that the number of background muons from hadron decay is reduced to a minimum, greatly lowering the chances of detecting two decay muons in time coincidence. The system described below has been optimized to give as large an acceptance as possible, consistent with sufficient momentum resolution to distinguish J/ψ from ψ'.

7.2 Absorber

We plan to absorb most photoproduced hadrons and photons using alumina (aluminum dioxide, Al_2O_3) placed just downstream of the target to minimize the number of muons from pion and kaon decays. Alumina was chosen because of the relatively low number of radiation lengths per interaction length, affordable cost, and its high density. Studies with GEANT indicate that a length of 2.2 m is sufficient to meet our goal of less than 80 hits per

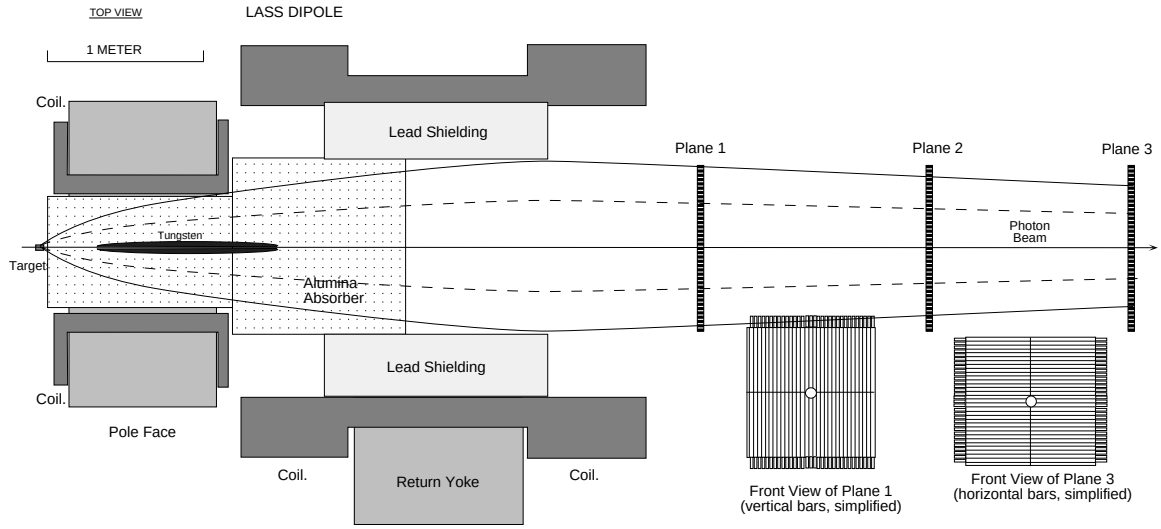

Figure 6: Overall plan view of the main components of the spectrometer. The first dipole downstream of the target will be filled with alumina and tungsten for absorbing particles that are not muons. The second dipole is from the LASS experiment. A simplified view of one of the detector planes is shown (about 1/2 of the fingers are shown). The solid (dashed) lines are typical muon pair decays from a J/ψ produced with $E_\gamma = 15$ GeV (35 GeV).

beam spill in the first detector plane. The rates are lower in the second and third detector planes. The magnetic field in the LASS dipole is useful in sweeping away most of the low momentum particles that emerge from the alumina. The GEANT studies show a higher rate of photons and neutrons hitting the front detector plane, but scaled by their detection efficiency, the singles rates will still be dominated by the charged particles. The studies were done assuming commercially available bricks with a density of 3.6 gm/cm^2, and 90% purity (the remaining material is mainly silicon dioxide).

7.3 Spectrometer

The spectrometer layout is shown in Fig. 6. There are two dipole magnets, operating with the same polarity. For the large opening angle (typically 600 mr) between muons from low energy J/ψ's, this helps to capture pairs by bending both muons towards the beam pipe. The two solid lines show the trajectories of a typical J/ψ decay for $E_\gamma = 15$ GeV, while the dashed lines are for $E_\gamma = 35$ GeV.

The first dipole is an existing 29D32 magnet, which has a 25.4 cm gap and effective length of about 1 m. Running at full current, we expect an integrated field of 22 kG-m for this magnet. The width between the coils of ± 36 cm is large enough to accommodate most J/ψ decays. The gap is not quite large enough to match the acceptance of the second dipole and the detectors, so that the small number of muons passing through the magnetized iron of the pole tips will suffer some additional multiple scattering, with a typical 10% to 20% increase in J/ψ mass resolution.

This gap will be filled with alumina in the good signal region corresponding to $\theta > 40$ mr. The portion corresponding to smaller angle tracks will be filled with tungsten to absorb the large number of Bethe-Heitler electron/positron pairs created in the target, and to provide maximum energy loss from the muon pairs. Our studies show only a small loss in acceptance for J/ψ decays by excluding the region $\theta < 40$ mr. We have estimated the number of J/ψ particles produced by the electron/positrons swept into the tungsten, and expect rates varying from 1% to 15% of the rate from the target itself, depending on photon energy and target thickness. They will be easily distinguished from J/ψ's produced in the target because they will make a smooth background under the energy peak corresponding to coherent bremsstrahlung photons. A vertical (non-bend plane) tracking cut may also be useful in rejecting these events.

An evacuated cylindrical hole in the absorber will allow the photon beam to pass through. The hole will be made as small as possible consistent with an acceptable of level from tails in the photon position distribution (7 to 10 mm diameter).

The second dipole is the 70D43 LASS dipole [43]. This dipole has two very large sets of coils arranged in a configuration that limits the useful vertical opening to about ± 55 cm over the 2.8 m distance between the mirror plates. The pole face is 109 cm long, and the gap is 102 cm. We plan to add shims to reduce the gap to about ± 45 cm to match the acceptance to that determined by the magnet coils, and to get a higher integrated field. The previously used 5 MW power supply is no longer available, but with this reduced gap, and using two existing 1.6 MW supplies in parallel running at 4000 amps, we expect to obtain an integrated field strength of 25 kG-m. We plan to remove the mirror plates to gain additional integrated field strength, and to allow the two dipoles to be placed closer together.

7.4 Detectors

Tracking of the muons will be done using planes of scintillator hodoscopes connected to multi-hit TDC's. The fine granularity and good timing of this type of system are needed to match hits from muon tracks that will occur on average every 10 to 30 nsec. We plan to use three planes of hodoscopes (see Fig. 6), segmented into top and bottom halves for the horizontal readout, and left and right halves for the vertical readout. This is done to reduce the random hit rate per finger, and to reduce the spread in signal height from attenuation of the light in the scintillator.

For measurements in the bend plane (horizontal), two sub-planes of 1.5 cm average width scintillator fingers will be used, giving an effective resolution of 0.15 cm. The sub-planes will use the 2/3 overlap strategy that worked well in E155. Positions in the non-bend plane (vertical) will be measured with horizontal fingers, each with 2 cm width, but with only a single sub-plane per plane, giving a position resolution of 0.7 cm. This gives a vertical angle resolution that is good enough to distinguish muons originating from the target from most random background from hadronic interactions in the absorber. Table 7 lists the overall dimensions of each plane, as well as the number of hodoscope fingers needed.

We plan to read out each finger with small PMTs, most of which can be taken from the

Plane	x (cm)	y (cm)	fingers
1	± 60	± 60	300
2	± 55	± 80	300
3	± 50	± 100	300
Total			900

Table 7: Dimensions of each scintillator plane and number of fingers.

existing E155 hodoscope arrays. The front plane will be 50 cm beyond the end of the LASS coils, where the magnetic field should be low enough that adequate magnetic shielding can be fabricated.

The signals from each hodoscope will pass through a discriminator and into a multi-hit TDC with 0.5 nsec granularity and leading edge readout, as was done in E155. Pulse widths are < 7 ns with TDC dead times of about 11 ns.

A similar system of scintillator hodoscopes was used in recent experiments E154 and E155. Scaling to the present proposal, we feel confident that the proposed system will be able to reliably track an expected rate of several high p_T muons passing through all three hodoscope planes per spill, and hit rates of up to 100 per plane per 500 nsec beam pulse from hadronic punch through particles (these mainly affect planes 1 and 2), and low p_T muons from pion decay, kaon decay, and Bethe-Heitler pairs. The muons with $p_T < 0.5$ rarely pass through the active areas of all three detector planes, due to the combination of spectrometer optics and the separation between detectors planes.

7.5 Acceptance and Resolution

A simple model of the spectrometer has been used to determine the expected performance. The effects of multiple scattering in the absorber and detectors, energy loss (and fluctuations) in the absorber, photon beam size, target length, and detector granularity have been taken into account. A realistic sample of J/ψ and ψ' particles was generated for each photon energy assuming the total cross sections on hydrogen measured at SLAC, a t distribution of e^{3t}, and no A-dependence to the incoherent quasi-elastic cross section per nucleon. Muon pairs were then generated using the known $1 + cos^2\theta^*$ distribution. The fraction of events for which both muons pass through all three detector planes is shown in Table 8 for both J/ψ and ψ'. The acceptance increases rapidly with energy due to the small opening angles between the muons.

The most stringent requirement on spectrometer resolution is set by the desire to distinguish J/ψ (mass 3.1 GeV) and ψ' (mass 3.7 GeV) decays. The expected ratio of branching fraction times cross section is about 0.03 ψ' per J/ψ, leading to a desired mass resolution of 0.14 GeV or better to avoid the tail of the J/ψ washing out the ψ' peak. As seen in Table 8, the spectrometer meets this goal. Using this mass resolution, we have calculated the number of Bethe-Heitler muon pairs [42] under the mass peaks and estimate backgrounds of less than 15% for the J/ψ and 25% for the ψ'. Elastic, quasi-elastic, and inelastic contributions were taken into account. The predicted mass spectra for beryllium are shown for 15 GeV

and 35 GeV photons in Fig. 7. The spectra look very similar for the higher Z targets, because the elastic Bethe-Heitler contributions are very small at these beam energies, due to the large values of t_{min} compared to experiments at higher energies. To minimize the Bethe-Heitler to J/ψ ratio, we have imposed two useful cuts on each muon: $\theta > 40$ mr, and $P > 2.5$ GeV. These cuts result in only a small loss of J/ψ decays.

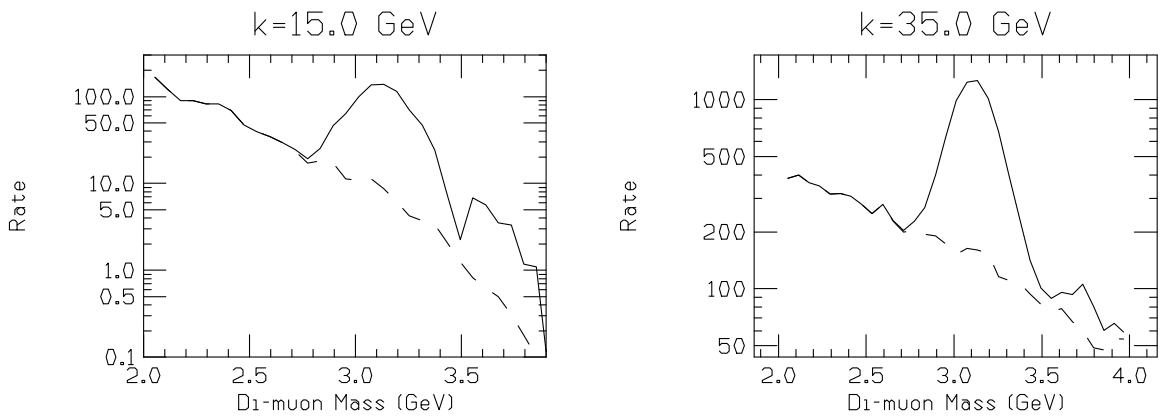

Figure 7: Predicted di-muon mass spectra for 15 GeV and 35 GeV photons. The dashed curve shows the sum of elastic, quasi-elastic, and inelastic Bethe-Heitler contributions that pass through the detectors and the additional cuts described in the text.

The muon pair energy resolution varies from 0.4 to 1.4 GeV for photon energies of 15 to 35 GeV. This is a good match to the width of the coherent bremsstrahlung peaks (see Fig. 5). The p_T^2 resolution is quite good at about 0.1 GeV^2. We cannot measure t directly without monochromatic photons, but in practice $p_T^2 \approx -t$, so this variable can be used to distinguish coherent, quasi-elastic, and inelastic contributions. The expected p_T^2 resolution is quite adequate to make these separations.

Peak Photon Energy (GeV)	15.0	25.0	35.0
J/ψ Mass Resolution (GeV)	0.120	0.127	0.142
J/ψ Energy Resolution (GeV)	0.54	1.04	1.80
J/ψ p_T^2 Resolution (GeV^2)	0.09	0.11	0.14
J/ψ Acceptance	0.07	0.17	0.24
ψ' Acceptance	0.01	0.16	0.23

Table 8: Acceptance and resolutions expected at each of the primary photon energies.

8 Run Plan

We plan to take data at three primary beam energies (see Table 5), giving coherent photon peaks at 15, 25, and 35 GeV. At 25 and 35 GeV, we will reconstruct about 8000 clean quasi-elastic J/ψ events and 200 ψ' events on each of the four targets. At 15 GeV, we will

collect about 2000 clean J/ψ events on two nuclear targets. A clean event is defined as being within 7% of the energy of the photon coherent peak. As seen in Table 5, we will typically collect three times more quasi-elastic events that are not in the photon coherent peak. A substantial number of inelastic events will be collected as well, especially at the highest energies.

As seen in Table 5, it takes approximately 10 days per beam energy to meet our statistical goals, where a day has been defined to be 10^7 beam spills, the number obtained in one 24 hour period at 120 Hz and 100% beam delivery efficiency. Assuming that this experiment is running concurrently with PEP-II, we anticipate an efficiency of 50%, so that it will take approximately 2 months to complete the experiment at 120 Hz repetition rate.

For each nuclear target, we plan to measure $d\sigma/dt$ for J/ψ and ψ' photoproduction. Resonant events will first be selected from a cut on invariant mass for the J/ψ and ψ'. Corrections for Bethe-Heitler pairs and muon pairs resulting from hadronic decays will be made using a combination of measured data and Monte Carlo simulations to determine the t-distributions of the background under the J/ψ and ψ' peaks in the invariant mass spectrum. The cross sections for coherent, quasi-elastic and inelastic production can be separated by fitting $d\sigma/dt$ to three exponentials as has been done in previous experiments [4]. Although a simple p_T^2 cut would eliminate the coherent contribution, precisely separating quasi-elastic from inelastic will rely on a cut in $z = E_{j/\psi}/E_\gamma$. This will require comparisons of events at and below the coherent bremsstrahlung peak.

9 Request

We request two weeks of checkout time at low repetition rate, and 2 months of production data taking at 120 Hz (or four months at 60 Hz). We request the re-establishment of the photon beam capability as used in E78. This will involve re-installation of the goniometer, refurbishing the dump magnets, installing a 20 kW beam dump, and help in re-establishing the standard photon beam monitors. We request the use of the LASS dipole and a smaller dipole such as the 29D36, and resources to make some modifications. We do not plan to run the LASS dipole higher than 2.5 MW. We request resources to purchase the hodoscope scintillator fingers, with assembly planned to be done by the collaboration. We will need to increase the existing supply of PMT channels by several hundred to read out the hodoscopes. Most of the needed discriminators and TDC's are already available. Some upgrades to the E.S.A. DAQ system may be needed to handle an estimated data rate of up to 16 kB per spill (4000 TDC hits).

References

[1] U. Camerini, *et al.*, Phys. Rev. Lett. **35**(1975)483.

[2] B. Knapp, *et al.*, Phys. Rev. Lett. **34**(1975)1040.

[3] R.L. Anderson *et al.*, Phys. Rev. Lett. **38**(1977)263.

[4] M.D. Sokoloff, *et al.*, Phys. Rev. Lett. **57**(1986)3003.

[5] C. Gerschel and J. Hüfner, Z. Phys. **C56**(1992)171.

[6] J. Hüfner and B.Z. Kopeliovich, Phys. Lett. **B426**(1998)154.

[7] M.C. Abreu, *et al.*, Phys. Lett. **B466**(1999)408.

[8] J. Hüfner, Yu.P. Ivanov, B.Z. Kopeliovich and A.V. Tarasov, hep-ph/0007111.

[9] Y.B. He, J. Hüfner and B.Z. Kopeliovich, Phys. Lett. **B477**(2000)93.

[10] L. Gerland, *et al.*, Phys. Rev. Lett. **81**(1998)762.

[11] G.R. Farrar, L.L. Frankfurt, M.I. Strikman and H. Liu, Phys. Rev. Lett. **64**(1990)2996.

[12] S.J. Brodsky and A. Mueller, Phys. Lett. **B206**(1988)685.

[13] B.Z. Kopeliovich and B.G. Zhakarov, Phys. Rev. D **44**(1991)3466.

[14] For a recent review see R. Vogt, Phys. Rep. **310**(1999)197.

[15] J. Hüfner, B. Kopeliovich, and A. Zamolodchikov, Z. Phys. **A357**(1997)113.

[16] E. Chudakov, *et al.*, draft proposal *Charm Studies at Threshold* for Jefferson Lab at 11 GeV.

[17] S.J. Brodsky and G.A. Miller, Phys. Lett. **B412**(1997)125.

[18] J.F. Martin, *et al.*, Phys. Rev. Lett. **34**(1975)288.

[19] B. Gittelman, *et al.*, Phys. Rev. Lett. **35**(1975)1616.

[20] T. Nash, *et al.*, Phys. Rev. Lett. **36**(1976)1233.

[21] M. Binkley, *et al.*, Phys. Rev. Lett. **48**(1982)73.

[22] B.H. Denby, *et al.*, Phys. Rev. Lett. **52**(1984)795.

[23] R. Barate, *et al.*, Z. Phys. **C33**(1987)505.

[24] P.L. Frabetti, *et al.*, Phys. Lett. **B316**(1993)197.

[25] J. Breitweg, *et al.*, Z. Phys. **C75**(1997)215; J. Breitweg, *et al.*, Z. Phys. **C76**(1997)599;

[26] S. Aid, *et al.*, Nucl. Phys. **B472**(1996)3; C. Adloff, *et al.*, Phys. Lett. **B421**(1998)385; C. Aldoff, *et al.*, Phys. Lett. **B483**(2000)23.

[27] J. Badier, *et al.*, Z. Phys. **C20**(1983)101.

[28] S. Katsanevas, *et al.*, Phys. Rev. Lett. **60**(1988)2121.

[29] S. Kartik, *et al.*, Phys. Rev. D **41**(1990)1.

[30] D.M. Alde, *et al.*, Phys. Rev. Lett. **66**(1991)133.

[31] Y. Alexandrov, *et al.*, Nucl. Phys. **B557**(1999)3.

[32] R.E. Tribble, *et al.*, Nucl. Phys. **A663-664**(2000)761c; M.J. Bennett and J.L Nagle, *Heavy Ion Physics From Bevalac to RHIC (Proc. Rel. Heavy Ion Symposium, APS Centennial Meeting 99)* ed. R. Seto, (World Sci.,Singapore, 1999) p. 247.

[33] J.J. Aubert, *et al.*, Phys. Lett. **B152**(1985)433; Nucl. Phys. **B213**(1983)1.

[34] E.L. Berger and D. Jones, Phys. Rev. D **23**(1981)1521.

[35] W. Kaune, *et al.*, Phys. Rev. D **11**(1975)478.

[36] R. Schwitters, SLAC-TN-70-32 (1970).

[37] G. Miller and D. Walz, SLAC-PUB-1297.

[38] D. Luckey and R. Schwitters, Nucl. Instr. Meth. **81**(1970)164.

[39] G. Diambrini Palazzi, Rev. Mod. Phys. **40**(1968)611.

[40] R. Jones, http://zeus.phys.uconn.edu/halld/cobrems-7-97/

[41] R. F. Mozley and J. DeWire, Nuevo Cimento **27** (1983)1281.

[42] Y.S. Tsai, Rev. Mod. Phys. **46**(1974)815; Rev. Mod. Phys. **49**(1977)421 (E).

[43] SLAC Report 298, April 1986.